Strain-controlled fundamental gap and structure of bulk black phosphorus

Jie Guan,[1] Wenshen Song,[2] Li Yang,[2] and David Tománek[1,*]
[1]*Physics and Astronomy Department, Michigan State University, East Lansing, Michigan 48824, USA*
[2]*Department of Physics, Washington University in St. Louis, St. Louis, Missouri 63130, USA*
(Received 28 March 2016; published 11 July 2016)

We study theoretically the structural and electronic response of layered bulk black phosphorus to in-layer strain. *Ab initio* density functional theory (DFT) calculations reveal that the strain energy and interlayer spacing display a strong anisotropy with respect to the uniaxial strain direction. To correctly describe the dependence of the fundamental band gap on strain, we used the computationally more involved *GW* quasiparticle approach that is free of parameters and is superior to DFT studies, which are known to underestimate gap energies. We find that the band gap depends sensitively on the in-layer strain and even vanishes at compressive strain values exceeding ≈2%, thus suggesting a possible application of black P in strain-controlled infrared devices.

DOI: 10.1103/PhysRevB.94.045414

I. INTRODUCTION

Layered bulk black phosphorus (BP), discovered only a century ago [1], is a direct-gap semiconductor with an observed fundamental band gap [2–5] of 0.31–0.36 eV. Its electronic response distinguishes BP as favorable from other well-studied layered systems including semimetallic graphite and transition metal dichalcogenides (TMDs) such as MoS_2, which are indirect-gap semiconductors. Under compression, bulk BP has displayed an interesting change in its electronic and topological properties [6–8]. Similar to bulk BP, a much wider direct fundamental band gap is present in phosphorene monolayers and few-layer systems, suggesting promising applications in two-dimensional (2D) semiconductor electronics [9–11]. Whereas it is now well established that the gap displays a strong and anisotropic response to in-layer strain in phosphorene monolayers and few-layer systems [9–16], no dependable data are available for the corresponding response in the bulk system.

To fill in this missing information, we study theoretically the structural and electronic response of layered bulk black phosphorus to in-layer strain. Our *ab initio* density functional theory (DFT) calculations reveal that the strain energy and interlayer spacing display a strong anisotropy with respect to the uniaxial strain direction. To correctly describe the dependence of the fundamental band gap on strain, we used the computationally more involved *GW* quasiparticle approach that is free of parameters and is superior to DFT studies, which are known to underestimate gap energies. We find that the band gap depends sensitively on the in-layer strain and even vanishes at compressive strain values exceeding ≈2%, thus suggesting a possible application of black P in strain-controlled infrared devices.

II. COMPUTATIONAL TECHNIQUES

We utilize *ab initio* density functional theory (DFT) as implemented in the SIESTA [17] code to optimize the structure and to determine the structural response to in-plane strain. We used the Perdew-Burke-Ernzerhof (PBE) [18] exchange-correlation functional, norm-conserving Troullier-Martins pseudopotentials [19], and a double-ζ basis including polarization orbitals. The reciprocal space was sampled by a fine grid [20] of $8 \times 8 \times 4$ k points in the first Brillouin zone of the primitive unit cell containing eight atoms. We used a mesh cutoff energy of 180 Ry to determine the self-consistent charge density, which provided us with a precision in total energy of $\leqslant 2$ meV/atom. All geometries have been optimized using the conjugate gradient method [21], until none of the residual Hellmann-Feynman forces exceeded 10^{-2} eV/Å.

DFT calculations are not designed to reproduce the electronic band structure correctly. Even though the DFT band structure usually resembles observed results, the fundamental band gap is usually underestimated. The proper way to calculate the band structure without adjustable parameters involves solving the self-energy equation. We perform such calculations using the *GW* approximation [22] as implemented in the BerkeleyGW package [23], where the dynamical electronic screening is captured by the general plasmon pole model. [22] We have expanded the dielectric matrix in plane waves up to a cutoff energy of 10 Ry. The quasiparticle energies are determined by considering the lowest 158 unoccupied conduction bands and accounting for all higher-lying bands using the modified static-remainder approximation [24]. We prefer this state-of-the-art approach to computationally less involved hybrid DFT functionals such as HSE06 [25], which mix Hartree-Fock and DFT-PBE exchange-correlation energies using an adjustable parameter. We use single-shot G_0W_0 calculations with a $14 \times 10 \times 4$ k-point grid, which provide converged results for the self-energies and quasiparticle energy gaps in strained bulk black phosphorus.

III. RESULTS

A. Strain-induced structural changes

The optimum structure of bulk black phosphorus, as obtained by DFT-PBE calculations, is shown in Fig. 1(a). As seen in the bottom panel, individual layers in the layered structure are not flat due to the nonplanar sp^3 hybridization of

*tomanek@pa.msu.edu

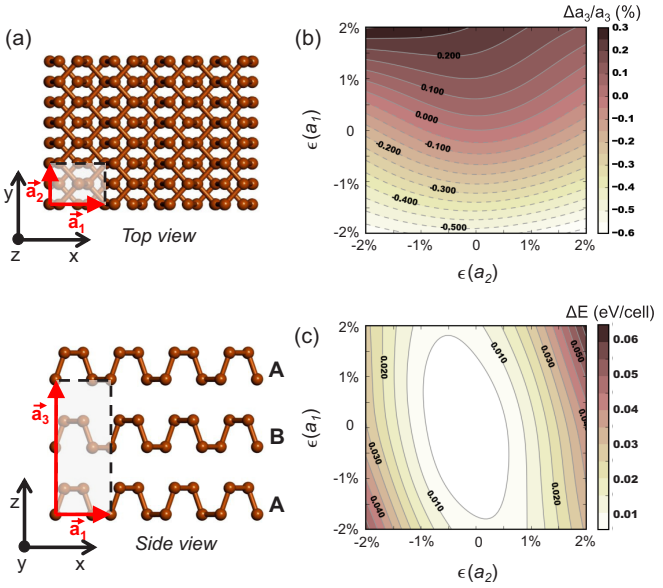

FIG. 1. (a) Ball-and-stick model of the structure of bulk black phosphorus in top and side views. (b) Fractional change of the interlayer distance a_3 as a function of the in-layer strain ϵ along the $\vec{a}_1$ and $\vec{a}_2$ directions. (c) Dependence of the strain energy ΔE per unit cell on the in-layer strain along the $\vec{a}_1$ and $\vec{a}_2$ directions.

the P atoms. The *AB* stacking is caused by displacing every other layer along the $\vec{a}_2$ direction, yielding an orthorhombic lattice spanned by the orthogonal lattice vectors $\vec{a}_1$, $\vec{a}_2$, and $\vec{a}_3$, with $\vec{a}_3$ extending over two interlayer distances. The covalent in-plane bonding is adequately described by DFT-PBE, as suggested by the agreement between the calculated lattice constants, a_1(PBE) = 4.53 Å and a_2(PBE) = 3.36 Å, and the experimental values [26] a_1(expt) = 4.38 Å and a_2(expt) = 3.31 Å. As indicated by recent quantum Monte Carlo studies [27], the nature of the weak interlayer interaction in bulk black phosphorus differs in a nontrivial manner from a van der Waals interaction. In view of this fact, the calculated value of the out-of-plane lattice constant a_3(PBE) = 11.15 Å agrees rather well with the observed value [26] a_3(expt) = 10.50 Å.

As a result of the weak interlayer interaction contrasting the strong in-layer covalent bonding, we do not expect the interlayer distance to change much when the lattice is subjected to in-layer strain. We considered both tensile and compressive in-layer strain ϵ up to 2%. Results for the fractional change $\Delta a_3/a_3$ for different strain combinations $\epsilon(\vec{a}_1)$,$\epsilon(\vec{a}_2)$ are presented in Fig. 1(b). The continuous contour plot is based on a cubic spline interpolation of a 5 × 5 grid of data points for different strain value combinations. These results, as well as our findings, suggest that the interlayer spacing changes much less than 1% for the strain range considered here. Such small changes in the interlayer distance are unlikely to be affected by the selection of the total energy functional, which plays only a minor role in the interlayer separation [27], and are consistent with very weakly coupled layers.

Our results in Fig. 1(b) indicate a trend that the interlayer distance increases by stretching and decreases by compressing the crystal along the soft, accordionlike $\vec{a}_1$ direction. In contrast, both stretching and compression along the stiffer $\vec{a}_2$ direction cause a reduction of the interlayer spacing. Even though these effects are small, they clearly reflect the anisotropy of the system. They translate to a very small negative Poisson ratio between the soft $\vec{a}_1$ in-layer direction and the $\vec{a}_3$ direction normal to the layers. The Poisson ratio between the hard $\vec{a}_2$ in-layer direction and the $\vec{a}_3$ direction is also very small in magnitude, but changes sign near $\epsilon(\vec{a}_2) = 0$. This definition of the Poisson ratio in the bulk differs from the "Poisson ratio" in a phosphorene monolayer, which relates the monolayer thickness to the in-layer strain and finds a negative value for that quantity [28].

With the optimum value of the interlayer spacing $a_{3,\mathrm{opt}}(\vec{a}_1,\vec{a}_2)$ for the different strain combinations at hand, we have calculated the strain energy ΔE as a function of $\epsilon(\vec{a}_1)$ and $\epsilon(\vec{a}_2)$ and present the results in Fig. 1(c). The prominently elliptical shape of the isoenergetic contours is another manifestation of the elastic anisotropy in the system. The observed tilt of the elliptical axes from the horizontal and vertical direction indicates a positive Poisson ratio $\nu_{21} = -d\epsilon(\vec{a}_2)/d\epsilon(\vec{a}_1) = 0.19$ within the phosphorene plane, indicating that stretching in one (in-plane) direction results in a lattice contraction in the normal (in-plane) direction. We find the lattice to be rather soft with respect to in-plane compression, since stretching by 2% even along the stiffer $\vec{a}_2$ direction requires an energy investment of only ≈0.06 eV per unit cell.

B. Strain-induced changes of the electronic structure

Results of our calculations for the electronic band structure and density of states (DOS) of unstrained and strained bulk black phosphorus are shown in Fig. 2. The DFT-PBE results, represented by the dashed red lines in Fig. 2(a),

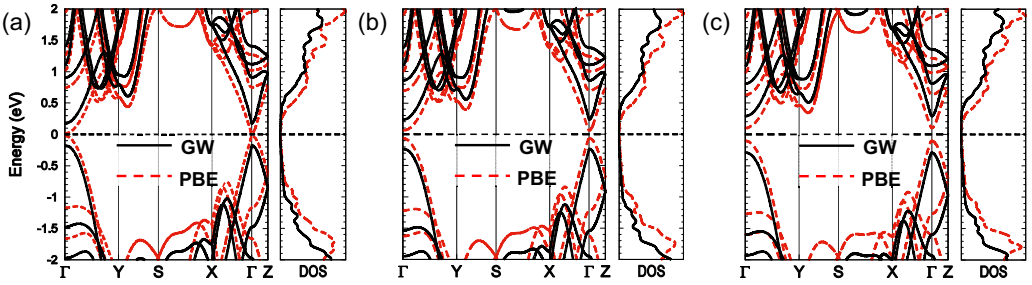

FIG. 2. Electronic band structure (left panels) and density of states (right panels) of bulk black phosphorus (a) without strain, (b) when stretched by 1% along the $\vec{a}_1$ direction, and (c) when stretched by 2% along the $\vec{a}_1$ direction. *GW* results are shown by the solid black lines. DFT-PBE results, which underestimate the band gap, are shown by the dashed red lines.

predict an extremely small direct fundamental band gap value $E_g(\text{PBE}) \approx 0.05$ eV for unstrained bulk black phosphorus. The band gap is becoming larger in the strained structures by stretching along the $\vec{a}_1$ direction. As mentioned before, the DFT results are known to substantially underestimate the band gap in semiconductors. Band structure results obtained using the more proper *GW* approach are represented by the solid black lines in Fig. 2(a). These data suggest a larger quasiparticle band gap $E_g(\text{qp}) \approx 0.35$ eV in unstrained bulk black phosphorus, very close to the published value based on *GW* calculations [29,30] and to the observed value [2] of ≈0.33 eV.

Differences between quasiparticle spectra E_{qp} and DFT band structure results E_{PBE} are summarized in Fig. 3(a). As shown previously [22,31], the self-energy (or *GW*) correction is roughly represented by a "scissor operator," which would shift DFT-based valence states rigidly down and conduction states rigidly up by $\lesssim$0.2 eV in bulk black phosphorus, thus opening up the fundamental band gap.

A more precise comparison between the quasiparticle spectra and DFT eigenvalues reveals that the difference $E_{\text{qp}} - E_{\text{PBE}}$ does depend on the energy, but is independent of the crystal momentum **k**. We considered black phosphorus stretched by 1% along the soft $\vec{a}_1$ direction, which has a nonzero band gap in DFT-PBE, and displayed the correlation between quasiparticle energies E_{qp} and corresponding DFT eigenvalues E_{PBE} at selected high symmetry points in the Brillouin zone in Fig. 3(a). Besides the discontinuity at the Fermi level, we found that the quasiparticle energies display a linear relationship with DFT eigenvalues, given by

$$E_{\text{qp}}(\text{CB}) = 1.10 \times E_{\text{PBE}}(\text{CB}) + 0.11 \text{ eV}, \quad (1)$$

$$E_{\text{qp}}(\text{VB}) = 1.07 \times E_{\text{PBE}}(\text{VB}) - 0.18 \text{ eV}. \quad (2)$$

Assuming that the Fermi level defines zero energy, the linear relationship between E_{qp} and E_{PBE} is slightly different in the conduction band (CB) region, identified by $E_{\text{qp}} > 0$, and the valence band region, identified by $E_{\text{qp}} < 0$. Since *GW* energies have been calculated only at a few k points, we have used expressions (1) and (2) to generate the continuous *GW* band structure shown in Fig. 2.

Comparing DFT and GW values at different strains, we found that the modulation of the band gap $\Delta E_g(\text{PBE}) \approx \Delta E_g(\text{qp})$ is the same up to $\lesssim$0.01 eV in the strain range studied here. With the quasiparticle band gap of unstrained black phosphorus at hand, we thus can deduce the quasiparticle band gap in phosphorus subject to different strain values $\epsilon(\vec{a}_1)$ and $\epsilon(\vec{a}_2)$ combining the DFT band gap values $E_g(\text{PBE})$ with Eqs. (1) and (2). Our results, based on a cubic spline interpolation of a 5×5 grid of data points, are shown in Fig. 3(b).

Our results indicate that, within the range $|\epsilon| \lesssim 2\%$ of strain applied along the $\vec{a}_1$ and $\vec{a}_2$ direction, the band gap E_g of bulk black phosphorus varies smoothly between 0.05 and 0.70 eV. Independent of the in-plane strain direction, E_g increases upon stretching and decreases upon compression. Noticing the nearly equidistant spacing between the contour lines in Fig. 3(b), we can extrapolate to larger strains and expect the band gap to close at compressive strains along both

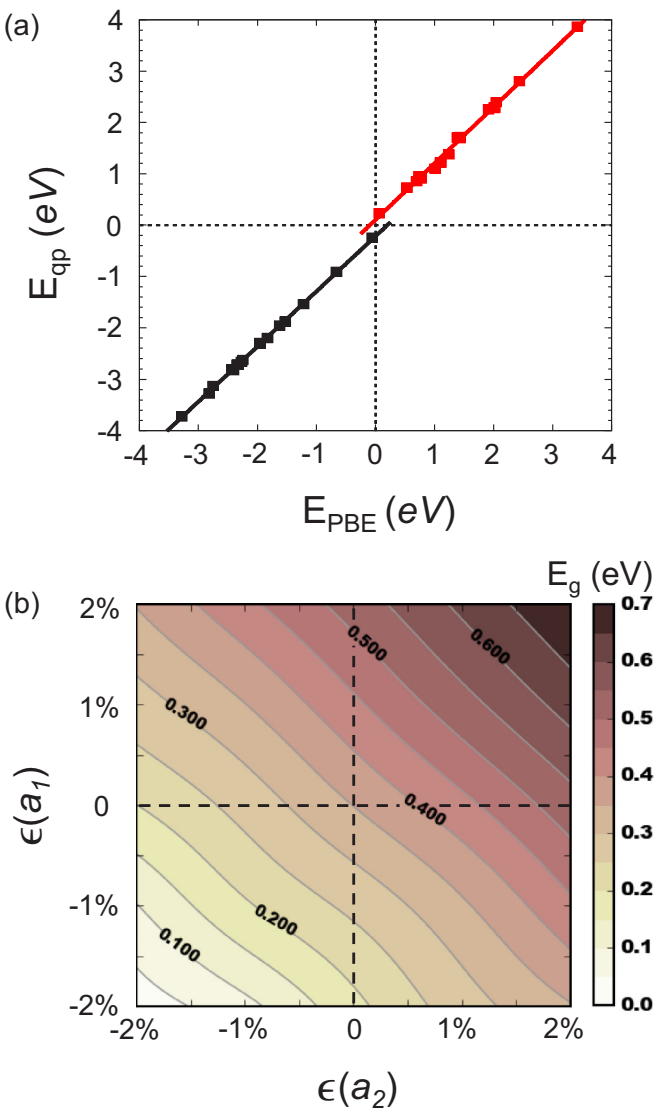

FIG. 3. (a) Correlation between quasiparticle (*GW*) energies E_{qp} and Kohn-Sham energy values E_{PBE}, obtained using the DFT-PBE functional, for states along high symmetry lines in the Brillouin zone. The straight lines in the valence and conduction band regions are drawn to guide the eye. The results represent bulk black phosphorus subject to strain values $\epsilon(\vec{a}_1) = 1\%$ and $\epsilon(\vec{a}_2) = 0$. The Fermi level is at zero energy. (b) Dependence of the quasiparticle (*GW*) electronic band gap E_g on the in-layer strain applied along the $\vec{a}_1$ and $\vec{a}_2$ directions.

$\vec{a}_1$ and $\vec{a}_2$ directions exceeding 2%. We have also identified a nearly linear dependence of E_g on the interlayer spacing and found that a 1% increase in the interlayer separation opens the gap by an additional 0.02 eV.

So far, much less attention has been paid to the moderate 0.3 eV band gap of bulk BP than to 2 eV wide direct band gap of a phosphorene monolayer [9]. The interlayer coupling in bulk BP, which is responsible for the large difference in the band gap, displays a nontrivial character [27]. Therefore, it has not been clear *a priori* if previously reached conclusions for the band gap dependence on uniaxial in-layer strain in a phosphorene monolayer will also be applicable

to the bulk system. There is an independent, more practical concern about band gap modulation in BP systems by strain. Pristine phosphorene monolayers and few-layer systems are very unstable under ambient conditions [32–34] and must be capped, typically by sandwiching in between inert *h*-BN layers to remain useful [35]. It is unclear if applying in-layer strain will not destroy the rigid capping layer before reaching desirable strain values in the enclosed phosphorene. This limitation applies to a much lesser degree to bulk black phosphorus, which is chemically much more stable and thus can be handled more easily in the experiment.

The sensitivity of the band gap to the in-layer strain suggests to use bulk or multilayer black phosphorus in infrared devices tunable by strain. Optical measurements should be able to reveal the band gap value discussed here, since observed optical spectra should not be modified by excitonic states due to the negligibly small exciton binding energy in bulk black phosphorus [29].

IV. SUMMARY AND CONCLUSIONS

In summary, we have studied theoretically the structural and electronic response of layered bulk black phosphorus to in-layer strain. *Ab initio* density functional theory (DFT) calculations reveal that the strain energy and interlayer spacing display a strong anisotropy with respect to the uniaxial strain direction. To correctly describe the dependence of the fundamental band gap on strain, we used the computationally more involved *GW* quasiparticle approach that is free of parameters and superior to DFT studies, which are known to underestimate gap energies. We found that the main difference between *GW* quasiparticle energies E_{qp} and DFT eigenvalues E_{PBE} is a discontinuity at the Fermi level and have identified the relationship between E_{qp} and E_{PBE} in the valence and conduction band regions. Similar to a phosphorene monolayer, we found that the band gap depends sensitively on the in-layer strain and even vanishes at compressive strain values exceeding $\approx 2\%$, thus suggesting a possible application of black P in strain-controlled infrared devices.

ACKNOWLEDGMENTS

J.G. and D.T. acknowledge the hospitality of Fudan University, where this study was initiated, and useful discussions with Yuanbo Zhang. We are also grateful to Garrett B. King for adapting the contour plot code and for useful discussions. J.G. and D.T. acknowledge financial support from NSF/AFOSR EFRI 2-DARE Grant No. EFMA-1433459. W.S. and L.Y. acknowledge support from NSF Grant No. EFRI-2DARE-1542815 and NSF CAREER Grant No. DMR-1455346. Computational resources have been provided by the Michigan State University High Performance Computing Center and the Stampede of Teragrid at the Texas Advanced Computing Center (TACC) through XSEDE.

[1] P. W. Bridgman, Two new modifications of phosphorus, J. Am. Chem. Soc. **36**, 1344 (1914).
[2] R. W. Keyes, The electrical properties of black phosphorus, Phys. Rev. **92**, 580 (1953).
[3] D. Warschauer, Electrical and optical properties of crystalline black phosphorus, J. Appl. Phys. **34**, 1853 (1963).
[4] S. Narita, Y. Akahama, Y. Tsukiyama, K. Muroa, S. Moria, S. Endo, M. Taniguchi, M. Seki, S. Suga, A. Mikuni, and H. Kanzaki, Electrical and optical properties of black phosphorus single crystals, Physica B+C **117-118**, 422 (1983).
[5] Y. Maruyama, S. Suzuki, K. Kobayashi, and S. Tanuma, Synthesis and some properties of black phosphorus single crystals, Physica B+C **105**, 99 (1981).
[6] Y. Akahama, S. Endo, and S. Narita, Electrical properties of single-crystal black phosphorus under pressure, Physica B+C **139**, 397 (1986).
[7] R. Fei, V. Tran, and L. Yang, Topologically protected Dirac cones in compressed bulk black phosphorus, Phys. Rev. B **91**, 195319 (2015).
[8] Z. J. Xiang, G. J. Ye, C. Shang, B. Lei, N. Z. Wang, K. S. Yang, D. Y. Liu, F. B. Meng, X. G. Luo, L. J. Zou, Z. Sun, Y. Zhang, and X. H. Chen, Pressure-Induced Electronic Transition in Black Phosphorus, Phys. Rev. Lett. **115**, 186403 (2015).
[9] H. Liu, A. T. Neal, Z. Zhu, Z. Luo, X. Xu, D. Tománek, and P. D. Ye, Phosphorene: An unexplored 2D semiconductor with a high hole mobility, ACS Nano **8**, 4033 (2014).
[10] Z. Zhu and D. Tománek, Semiconducting Layered Blue Phosphorus: A Computational Study, Phys. Rev. Lett. **112**, 176802 (2014).
[11] L. Li, Y. Yu, G. J. Ye, Q. Ge, X. Ou, H. Wu, D. Feng, X. H. Chen, and Y. Zhang, Black phosphorus field-effect transistors, Nat. Nanotechnol. **9**, 372 (2014).
[12] A. S. Rodin, A. Carvalho, and A. H. Castro Neto, Strain-Induced Gap Modification in Black Phosphorus, Phys. Rev. Lett. **112**, 176801 (2014).
[13] R. Fei and L. Yang, Strain-engineering the anisotropic electrical conductance of few-layer black phosphorus, Nano Lett. **14**, 2884 (2014).
[14] X. Peng, Q. Wei, and A. Copple, Strain-engineered direct-indirect band gap transition and its mechanism in two-dimensional phosphorene, Phys. Rev. B **90**, 085402 (2014).
[15] D. Çakır, H. Sahin, and F. M. Peeters, Tuning of the electronic and optical properties of single-layer black phosphorus by strain, Phys. Rev. B **90**, 205421 (2014).
[16] W. Ju, T. Li, H. Wang, Y. Yong, and J. Sun, Strain-induced semiconductor to metal transition in few-layer black phosphorus from first principles, Chem. Phys. Lett. **622**, 109 (2015).
[17] E. Artacho, E. Anglada, O. Dieguez, J. D. Gale, A. Garcia, J. Junquera, R. M. Martin, P. Ordejon, J. M. Pruneda, D. Sanchez-Portal, and J. M. Soler, The SIESTA method; developments and applicability, J. Phys.: Condens. Matter **20**, 064208 (2008).
[18] J. P. Perdew, K. Burke, and M. Ernzerhof, Generalized Gradient Approximation Made Simple, Phys. Rev. Lett. **77**, 3865 (1996).
[19] N. Troullier and J. L. Martins, Efficient pseudopotentials for plane-wave calculations, Phys. Rev. B **43**, 1993 (1991).
[20] H. J. Monkhorst and J. D. Pack, Special points for Brillouin-zone integrations, Phys. Rev. B **13**, 5188 (1976).

[21] M. R. Hestenes and E. Stiefel, Methods of conjugate gradients for solving linear systems, J. Res. Natl. Bur. Stand. **49**, 409 (1952).

[22] M. S. Hybertsen and S. G. Louie, Electron correlation in semiconductors and insulators: Band gaps and quasiparticle energies, Phys. Rev. B **34**, 5390 (1986).

[23] J. Deslippe, G. Samsonidze, D. A. Strubbe, M. Jain, M. L. Cohen, and S. G. Louie, BerkeleyGW: A massively parallel computer package for the calculation of the quasiparticle and optical properties of materials and nanostructures, Comput. Phys. Commun. **183**, 1269 (2012).

[24] J. Deslippe, G. Samsonidze, M. Jain, M. L. Cohen, and S. G. Louie, Coulomb-hole summations and energies for *GW* calculations with limited number of empty orbitals: A modified static remainder approach, Phys. Rev. B **87**, 165124 (2013).

[25] A. V. Krukau, O. A. Vydrov, A. F. Izmaylov, and G. E. Scuseria, Influence of the exchange screening parameter on the performance of screened hybrid functionals, J. Chem. Phys. **125**, 224106 (2006).

[26] R. Hultgren, N. S. Gingrich, and B. E. Warren, The atomic distribution in red and black phosphorus and the crystal structure of black phosphorus, J. Chem. Phys. **3**, 351 (1935).

[27] L. Shulenberger, A. D. Baczewski, Z. Zhu, J. Guan, and D. Tománek, The nature of the interlayer interaction in bulk and few-layer phosphorus, Nano Lett. **15**, 8170 (2015).

[28] J.-W. Jiang and H. S. Park, Negative Poisson's ratio in single-layer black phosphorus, Nat. Commun. **5**, 4727 (2014).

[29] V. Tran, R. Soklaski, Y. Liang, and L. Yang, Layer-controlled band gap and anisotropic excitons in few-layer black phosphorus, Phys. Rev. B **89**, 235319 (2014).

[30] A. N. Rudenko, S. Yuan, and M. I. Katsnelson, Toward a realistic description of multilayer black phosphorus: From *GW* approximation to large-scale tight-binding simulations, Phys. Rev. B **92**, 085419 (2015).

[31] S. B. Zhang, D. Tománek, Marvin L. Cohen, S. G. Louie, and M. S. Hybertsen, Evaluation of quasiparticle energies for semiconductors without inversion symmetry, Phys. Rev. B **40**, 3162 (1989).

[32] A. Favron, E. Gaufres, F. Fossard, A.-L. Phaneuf-L'Heureux, N. Y.-W. Tang, P. L. Levesque, A. Loiseau, R. Leonelli, S. Francoeur, and R. Martel, Photooxidation and quantum confinement effects in exfoliated black phosphorus, Nat. Mater. **14**, 826 (2015).

[33] J. D. Wood, S.A. Wells, D. Jariwala, K.-S. Chen, E. Cho, V. K. Sangwan, X. Liu, L. J. Lauhon, T. J. Marks, and M. C. Hersam, Effective passivation of exfoliated black phosphorus transistors against ambient degradation, Nano Lett. **14**, 6964 (2014).

[34] T. Yang, B. Dong, J. Wang, Z. Zhang, J. Guan, K. Kuntz, S. C. Warren, and D. Tománek, Interpreting core-level spectra of oxidizing phosphorene: Theory and experiment, Phys. Rev. B **92**, 125412 (2015).

[35] X. Chen, Y. Wu, Z. Wu, Y. Han, S. Xu, L. Wang, W. Ye, T. Han, Y. He, Y. Cai, and N. Wang, High-quality sandwiched black phosphorus heterostructure and its quantum oscillations, Nat. Commun. **6**, 7315 (2015).